Int. J. Heat Mass Transfer. Vol. 17, pp. 1517–1526. Pergamon Press 1974. Printed in Great Britain

EXPERIMENTAL VERIFICATION OF THERMAL REMOTE SENSING METHOD FOR RECOVERING TEMPERATURE DISTRIBUTION IN GLASS

G. L. GRONINGER*, R. VISKANTA and R. E. CHUPP†
Heat Transfer Laboratory, School of Mechanical Engineering, Purdue University, West Lafayette, Indiana 47907, U.S.A.

(*Received* 29 *January* 1974 *and in revised form* 17 *May* 1974)

Abstract—The thermal remote sensing method for recovering the temperature distribution in glass from spectral emission data is examined experimentally. An analytical model is formulated and the desired temperature distribution is obtained using an optimization scheme which determines the temperature profile in the form of a polynomial or a set of discrete points. In order to evaluate the accuracy and validity of the thermal remote sensing method, the recovered temperatures are compared with independent measurements using surface thermocouples and a Mach–Zehnder interferometer. Experimental results are reported for fused silica (Corning Code 7940) glass samples using a Perkin–Elmer spectrometer to measure the spectral radiant energy emerging from the layer of glass. Opaque (high and low emittance) boundary conditions at the heated surface of the glass were considered. Temperatures in the range from 500 to about 900 K were examined. Spectral emission data between 3·3 and 4·8 μm were used in recovering the temperature distribution in the glass samples. The results showed that the recovered and interferometrically measured temperature profiles agreed well, with the maximum deviation never exceeding approximately 2 per cent.

NOMENCLATURE

- C_j, coefficients defined in equation (7);
- c_0, velocity of light in free space;
- h, Planck's constant;
- I_ν, spectral intensity of radiation;
- $I_{b\nu}$, Planck's function defined as $2h\nu^3/\{c_0^2[\exp(h\nu/kT)-1]\}$;
- k, Boltzmann's constant;
- L, thickness of layer;
- N, number of independent observations;
- n, index of refraction;
- T, temperature;
- y, depth.

Greek symbols

- β, function defined as $[1-\rho_{1\nu}(\mu)\rho_{2\nu}(\mu)\exp(-2\tau_{0\nu}/|\mu|)]^{-1}$;
- ε, emittance;
- θ, angle between normal and pencil of radiation;
- κ, absorption coefficient;
- λ, wavelength;
- μ, direction cosine, $\mu = \cos\theta$;
- μ', direction cosine in surrounding media, $\mu' = \cos\theta'$;
- ν, frequency;
- ξ, dimensionless depth, y/L;
- ρ, reflectance;
- Υ_ν, transmission function defined by equation (6);
- $\tau_{0\nu}$, optical thickness of layer defined as $\int_0^L \kappa_\nu(y)\,dy$.

Subscripts

- i, refers to ith independent observation;
- ref, refers to reference condition;
- 0, refers to external media;
- 1, refers to interface between semitransparent solid and the surrounding media;
- 2, refers to interface between semitransparent solid and opaque material;
- ν, refers to frequency.

Superscripts

- $+$, positive μ direction
- $-$, negative μ direction.

INTRODUCTION

INHERENT experimental difficulties are associated with measurement of the temperature distribution in semitransparent and diathermanous materials under dynamic conditions. For example, measurement and

*Presently at Gulf Atomic Company, San Diego, California 92138, U.S.A.

†Presently at Detroit Diesel Allison, Division of General Motors Corporation, Indianapolis, Indiana 46206, U.S.A.

control of temperature is essential in the efficient manufacture and utilization of glass products. Two standard types of temperature measurement systems for semitransparent and diathermanous materials such as glass are probes (primarily thermocouples) and radiation thermometry. However, the thermocouples distort the temperature field by conduction and respond to radiation other than local sources, thereby producing erroneous temperature results [1]. Radiation thermometers without an attached filter yield only an effective temperature for some unknown depth. Radiation thermometers are attractive because they can be placed remote to the medium sensed. Filters may be employed to make the thermometer sensitive to wavelengths only in certain narrow bands; however, various difficulties with thermometers have inhibited their general and broad application [2]. Optical techniques such as temperature-dependent attenuation of a He–Ne laser beam [3] and Mach–Zehnder interferometry [4] have also been employed. Unfortunately, the latter two methods are considered only as research tools rather than industrial diagnostic techniques.

This paper considers the spectral thermal remote sensing (inversion or spectral scanning) technique for determining the temperature distribution in semitransparent materials. The technique is an extension and generalization of radiation thermometry. Thermal remote sensing involves the use of a spectral sensor (spectrometer, radiometer with filters, etc.) to measure the natural emission from the medium and then recovering the temperature distribution by inversion of spectral emission data. The wavelength interval over which data is recorded is controlled by the spectral absorption characteristics and temperature of the medium and method of data inversion. This technique, although limited by the signal-to-noise level of the detection system at lower temperatures, is suited for thermal measurements since the radiation emerging from the medium is a function of the temperature distribution. The measurements can be made from remote locations providing the absorption due to the presence of the intervening media between the detector and the material is accounted for.

The theory and application of remote sensing techniques for gaseous radiation sources such as planetary and stellar atmospheres, plasmas, rocket exhaust plumes, etc., have been reviewed by Wang [5] and there is no need to repeat that survey. Attempts to measure temperature distribution in glass using data from two wavelength radiometers have been reported by Van Laethan *et al.* [6] and Beattie [7, 8]. An analysis for recovering the distribution in glass from remote spectral emission measurements has been presented by Chupp [9, 10].

The specific objective of this work is to experimentally verify the accuracy and validity of the thermal remote sensing method developed by Chupp. This is accomplished by comparing the recovered temperature profiles with independent measurements using Mach–Zehnder interferometer and surface thermocouples. For a critical comparison a well defined system is employed which utilizes a plane layer of fused silica (Corning Code 7940) glass as a test specimen. Emphasis in the paper is placed on the experiment and the results with a brief description of analysis and inversion technique. Experimental results are reported for several different temperature levels in the temperature ranging from 500 K to about 900 K for an opaque boundary condition (with a low and high emittance) at the heated face of the layer of glass.

ANALYSIS

Physical model and assumptions

The inversion procedure is best illustrated by applying it to a real system using the physical laws and geometry of that system. A schematic diagram of the physical model and coordinate system is shown in Fig. 1. A plane layer of glass bounded on one side by an opaque material is considered. The glass is assumed to be isotropic and homogeneous and able to absorb and emit, but not scatter, thermal radiation. The glass is also assumed to be in local thermodynamic equilibrium; therefore, Kirchhoff's and Planck's laws appropriately describe emission of radiation from the glass.

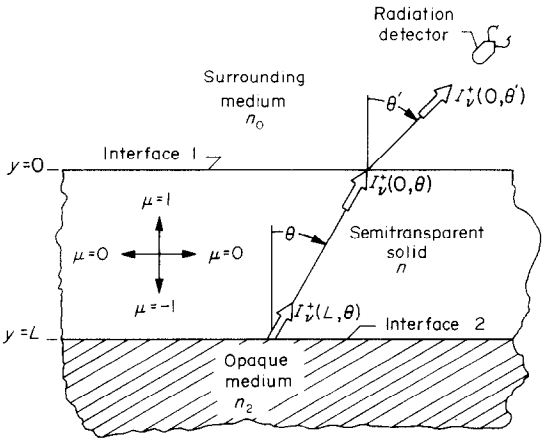

FIG. 1. Physical model and coordinate system.

The spectral intensity of radiation, $I_\nu^+(0,\theta')$, emerging from the layer as shown in Fig. 1 can be evaluated if the intensity just inside the material at the back face, $I_\nu^+(L,\theta)$ is known. Since the refractive index n_ν of the glass is usually much different than that of the surroundings and the opaque medium, the effect of

reflection at each of these interfaces must be included in $I_\nu^+(L,\theta)$. It is assumed that interfaces 1 and 2 in Fig. 1 are optically smooth and reflect specularly. Thus, Fresnel's equations of classical electromagnetic theory are appropriate to describe transmission and reflection of radiation characteristics of the interfaces.

Formulation of the problem

The basic principles of radiative transfer in semi-transparent media are well known [11]. Radiative transfer in glass is based on a fundamental equation resulting from a radiant energy balance on a pencil of radiation propagating in a given direction. For a one-dimensional, nonscattering, plane layer of glass the spectral intensity $I_\nu(y,\theta)$ defining the radiation field is governed by the equation of transfer

$$\cos\theta\frac{\mathrm{d}I_\nu}{\mathrm{d}y} = -\kappa_\nu[n_\nu^2 I_{b\nu}(y) - I_\nu(y,\theta)]. \quad (1)$$

This equation indicates that the spectral intensity $I_\nu(y,\theta)$ is increased by emission and decreased by absorption in the path length $\mathrm{d}y/\cos\theta$. The first term on the right of this equation accounts for emission while the second for absorption of radiation. It is convenient to divide $I_\nu(y,\theta)$ into two contributions: the intensity directed in the forward direction ($\mu=\cos\theta>0$) which is denoted by $I_\nu^+(y,\mu)$, and that directed in the negative direction ($\mu<0$) denoted by $I_\nu^-(y,\mu)$. Assuming that there is no radiation incident from an external source, the boundary conditions for equation (1) can be written as

$$I_\nu^-(0,\mu) = \rho_{1\nu}(\mu)I_\nu^+(0,\mu) \quad \text{for} \quad \mu<0 \quad (2)$$

and

$$I_\nu^+(L,\mu) = \varepsilon_{2\nu}(\mu)n_\nu^2 I_{b\nu}(T_2) + \rho_{2\nu}(\mu)I_\nu^-(L,\mu) \quad \text{for} \quad \mu>0. \quad (3)$$

Equation (1) with the boundary conditions (2) and (3) define the spectral intensity at any location within the layer. These equations can be solved for the intensity just inside the glass at interface 1, $I_\nu^+(0,\mu)$. From an energy balance on interface 1, the intensity emerging outwardly from the glass, $I_\nu^+(0,\mu')$, is related to the intensity just inside the glass by the relation

$$I_\nu^+(0,\mu') = [1-\rho_{1\nu}(\mu)](n_{0\nu}^2/n_\nu^2)I_\nu^+(0,\mu) \quad (4)$$

where direction cosines μ and μ' are related by Snell's law of refraction, $n_\nu\sin\theta = n_{0\nu}\sin\theta'$. From equations (1) through (4) the spectral intensity of radiation emerging outwardly from the glass becomes

$$I_\nu^+(0,\mu') = [1-\rho_{1\nu}(\mu)](n_{0\nu}/n_\nu)^2\beta_\nu(\mu) \times \{[1-\rho_{2\nu}(\mu)]n_\nu^2 I_{b\nu}(T_2)\Upsilon_\nu(L,0,\mu) + \int_0^L n_\nu^2 I_{b\nu}(y)[\Upsilon_\nu(y,0,\mu) + \rho_{2\nu}(\mu)\Upsilon_\nu(L,0,\mu)\Upsilon_\nu(L,y,\mu)]\kappa_\nu\,\mathrm{d}y/\mu\}, \quad \mu>0 \quad (5)$$

where the transmission function $\Upsilon_\nu(a,b,\mu)$ is defined as

$$\Upsilon_\nu(a,b,\mu) = \exp\left[-\int_b^a \kappa_\nu(\eta)\,\mathrm{d}\eta/\mu\right] \quad (6)$$

and where the factor $\beta_\nu(\mu)$ accounts for multiple internal reflection between interfaces 1 and 2.

Assuming that the spectral absorption coefficient κ_ν and Planck's function $I_{b\nu}[T(y)]$ are known and $I_\nu^+(0,\mu')$ is measured within experimental error, the problem is to recover the temperature distribution in the glass, i.e. $T(y)$, from equation (5) between $y=0$ and $y=L$. This involves measuring the spectral emerging intensity $I_\nu^+(0,\mu')$ with an appropriate instrument for N independent frequencies and/or directions and then recovering $T(y)$. The spectral directional reflection and transmission characteristics of interfaces 1 and 2 as well as the spectral optical properties (n_ν and κ_ν) of the semi-transparent material and their variation with temperature are assumed known in recovering $T(y)$.

Method of inversion

Inversion of a Fredholm integral equation of the first kind such as equation (5) encounters problems of instability, nonuniqueness, ill-conditioning and finite measurements. These difficulties are well recognized [5]. In an attempt to overcome some of these difficulties, a nonlinear optimization scheme has been adapted [9, 10]. This is a general procedure of inversion where *a priori* knowledge of the temperature distribution is not necessarily required and Planck's function need not be linearized. In the procedure developed the integral equation (5) is solved repeatedly with trial (assumed) temperature distributions in an attempt to recover the temperature distribution which best represents the spectral emission data. Two possible ways of representing the temperature distribution considered are: (1) a discrete set of points $T(\xi_j)$, and (2) a linear combination of functions, preferably orthogonal polynomials, such that

$$T/T_{\mathrm{ref}} = \sum_{j=1}^{m} C_j\psi_j(\xi), \quad 0\leqslant\xi\leqslant 1 \quad (7)$$

Legendre polynomials have been employed exclusively for ψ_j. Both of these methods have been used for representing the temperature distribution. The inversion procedure is described in detail by Chupp [9, 10].

EXPERIMENTS

General considerations

A critical check on the accuracy of the remote sensing method was made by comparing recovered temperature profiles with independent measurements. A Mach–Zehnder interferometer was employed to independently measure the temperature profile without interfering with the temperature and radiation fields or introducing

a radiation error. An interferometer can measure only a two-dimensional temperature field. Thus, any temperature variation in the glass in the direction of the interferometric beam should be minimized by reducing the edge losses from the glass specimen. Evacuation of the environment is an effective way of reducing edge losses by convection and conduction. The radiation edge losses were minimized using high reflectance coatings and shields.

The sample material had to meet several criteria. First, it had to be semitransparent in a frequency range which could be detected by spectrometer equipment available. Second, the sample should be transparent to radiation at the interferometric test beam frequency and have a refractive index which varies with temperature at this frequency. The sample should also be of high optical quality, workable to interferometric tolerance and durable with a low sensitivity to thermal stress. The latter stipulation implies a low coefficient of thermal expansion which has the additional advantage of reducing changes in the optical path due to expansion. Anderson *et al.* [4, 12] have developed an interferometric technique for temperature measurement in glass. They found that fused silica glass meets these criteria. In addition, fused silica glass has relatively well-known transport and optical properties (i.e. spectral absorption coefficient and spectral index of refraction).

Description of apparatus

Applications of the Mach–Zehnder interferometry to temperature studies are extensive and its principles well known [13]. As discussed by Anderson [4, 12], the change in the interference pattern (i.e. fringe shift) may be related to the temperature field through the index of refraction of the fused silica specimen. The interferometer system and the vacuum chamber used in the experiments have been described elsewhere [4], and only modifications of the system are discussed here. A schematic diagram of the test set-up is shown in Fig. 2.

A high density modular radiant heater (Research, Inc., Model 5208) was used as the heater source. The heater reflector and case body were water cooled, see Fig. 3. Two Sorensen power supplies provided the heater power. The heater unit was 0·241-m long and 0·076-m wide and employed six tungsten turbular quartz lamps (General Electric Co., Type T-3) in compact array. A 6·35-cm square and 0·635-cm thick copper plate was placed over the radiant heater to serve as the heating element. The copper plate was surrounded by lava insulation to provide stability and aid in maintaining a uniform face temperature. The test specimen was placed on the top and in direct contact with the heating element.

Thermocouples with 0·25-mm dia. leads were attached on bottom surface of the glass sample in order to reference the interferometer temperature profiles. Type K (Chromel–Alumel) thermocouples were used and all thermocouples were calibrated prior to installation.

A view port with a 5·08-cm dia. CaFl window as shown in Fig. 2 was installed at the top of the chamber to allow viewing of the glass sample to obtain the spectral emission data required for the inversion technique. CaFl was selected as the window material

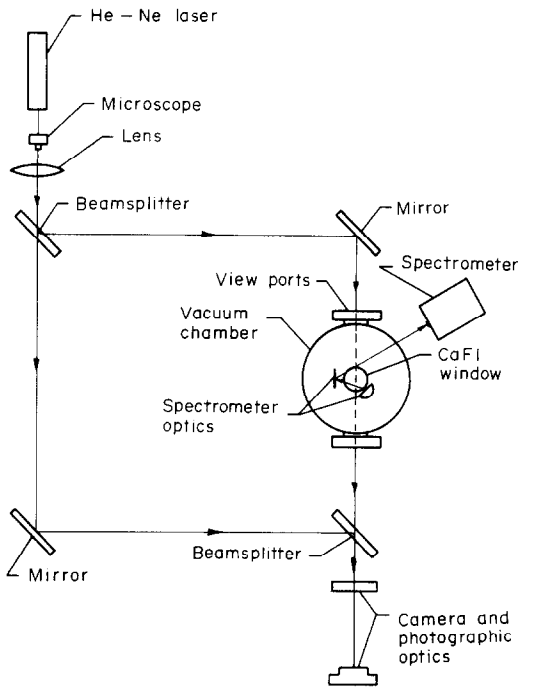

FIG. 2. Schematic diagram of the experimental apparatus.

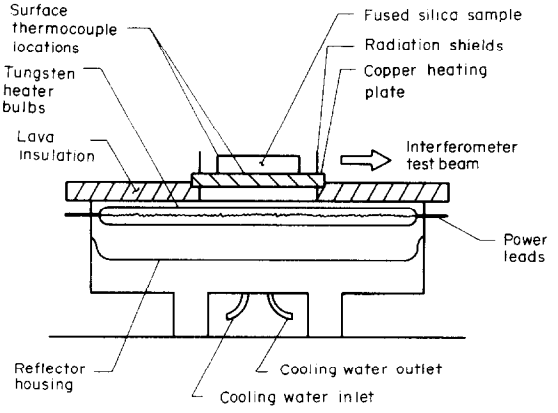

FIG. 3. Cross-sectional view of test assembly.

because it is transparent to radiation in the spectral range considered in the experiment.

Spectral emission from the sample was measured using a Perkin–Elmer Model 112 spectrometer. Fixed mirrors on the top of the vacuum chamber reflected radiation emerging from the sample to the slit of the spectrometer. During testing the spectrometer and optical path to the vacuum chamber window were purged with nitrogen to eliminate any gases having absorption bands in the spectral region of interest. Radiative flux emitted by the sample and incident on the slit was detected, amplified and recorded on an x–y plotter (Honeywell, Inc., Model 500) connected directly to the spectrometer.

Sample preparation

Corning Code 7940 fused silica glass 5·08-cm square and 1·27-cm thick, polished to interferometric tolerances, was used as the test sample. The size was selected to keep the interference fringe shift within resolvable limits while retaining a reasonable thickness to length ratio to minimize edge losses. Radiation losses from the edges of the glass were reduced by painting the edges with a low emittance gold paint (Liquid Bright Gold, Englehard Industries). The paint was cured at high temperature which left an opaque reflective gold film. A 6·35-mm window was left near the center of the sample to allow passage of the test beam. High emittance black paint (Pyromark High Temperature, Tempil Co.) and low emittance gold paint (Liquid Bright Gold) were coated on the bottom face to provide different boundary conditions. Both the black and gold coatings were observed to specularly reflect the visible radiation inside the sample and are therefore expected to be specular in the infrared. Edge losses were further reduced by positioning a silver foil reflection shield around the glass leaving only gaps for the interferometer test beam.

Experimental procedures and data reduction

A blackbody was installed *in situ* in the vacuum chamber to calibrate out factors such as the transmission characteristics of windows and the reflection of mirrors. The spectrometer readings could then be related to the known spectral radiation characteristics of the reference source.

After alignment of the spectrometer, the vacuum chamber was sealed and evacuated and the contents allowed to reach equilibrium. The interferometer was then adjusted to obtain the infinite fringe (i.e. uniform illumination). After steady state had been reached, the thermocouples were read and an interferogram photograph taken simultaneously. At this time the sample was scanned and spectral radiation emitted was recorded with the spectrometer and x–y plotter. The highest temperature level obtainable was limited by the fact that the black and gold coatings showed severe degradation at about 880 K.

Because the fringe density was relatively high ($\sim 10^2$ fringes/cm) magnification was required prior to photographing. The reading of the interferograms was accomplished with a coordinate microscope (Precision Tool and Instrument, Ltd., Vernier Microscope). By repeated reading of an interferogram, it was found that one tenth of a fringe could be resolved. The index of refraction data for fused silica were taken from Wray and Neu [14]. The local temperatures could be resolved within 0·3°C accounting for interferometric errors due to thermal distortion and refraction effects [12].

RESULTS AND DISCUSSION

General considerations

In order to examine the validity of the thermal remote sensing method over a wide range of physical parameters samples with opaque (high and low emittance) boundary conditions were studied. A range of temperatures was considered for each boundary condition to examine the accuracy of the thermal remote sensing method over as wide a temperature range as possible.

A single glass specimen of 1·27 cm thickness was used in the experiments. Spectral emission data were recorded in the wavelength range from 2·0 μm to 5·2 μm; however, only data in the wavelength range from 3·6 μm to 4·8 μm were used to obtain most experimental results. In this spectral region, fused quartz varies from being nearly transparent to opaque, i.e. it is semi-transparent. Spectral absorption coefficient data were taken from Wedding [15] and Edwards [16].

For all experimental results, spectral emission data were taken in the normal direction ($\mu' = 1$) relative to the glass surface. The temperature recovered using the inversion technique was constrained [10] to increase monotonically with the dimensionless distance (ξ).

Measured and recovered temperature profile results

The interferometrically measured and recovered temperature profiles for the low emittance boundary conditions (Liquid Bright Gold coating at the back face of the glass) for several different temperature levels are presented in Fig. 4 for both the polynomial and discrete point methods. Index of refraction data for gold were taken from the literature [17] to predict the reflection at interface 2.

High emittance boundary condition (Black Pyromark coating at the back face of the glass) results are presented for the polynomial and discrete point methods in Fig. 5. Normal spectral emittance data were taken from publications of the Thermophysical Properties and Research Center [18]. These data are

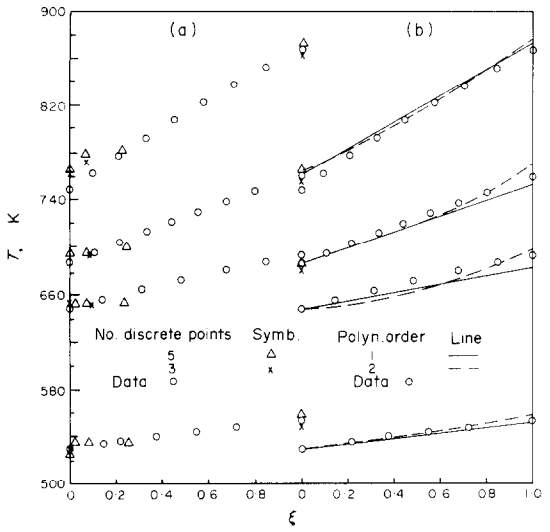

FIG. 4. Comparison of measured and recovered temperature profiles using discrete point (a) and Legendre polynomial (b) approaches; gold coating at the back face, $N = 10$, $\varepsilon \simeq 0{\cdot}06$, $3{\cdot}66\,\mu\text{m} \leqslant \lambda \leqslant 4{\cdot}75\,\mu\text{m}$, $1{\cdot}65 \leqslant \tau_{0\lambda} \leqslant 40{\cdot}71$.

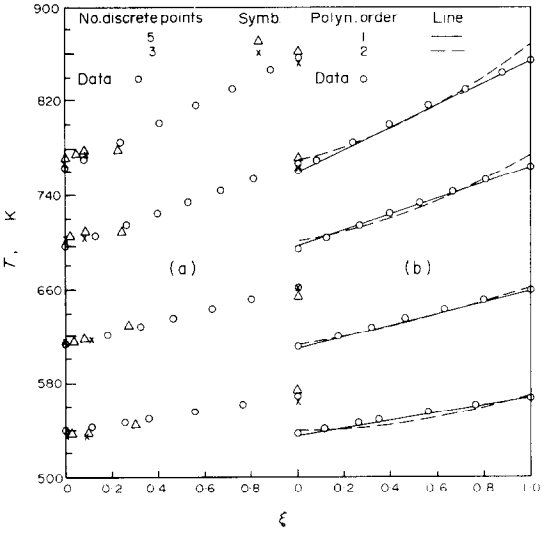

FIG. 5. Comparison of measured and recovered temperature profiles using discrete point (a) and Legendre polynomial (b) approaches; Pyromark black paint at the back face, $N = 10$, $\varepsilon \simeq 0{\cdot}80$, $3{\cdot}66\,\mu\text{m} \leqslant \lambda \leqslant 4{\cdot}75\,\mu\text{m}$, $1{\cdot}66 \leqslant \tau_{0\lambda} \leqslant 40{\cdot}70$.

for Pyromark emitting into air. Since this experiment deals with a Pyromark-fused silica interface, the published data had to be corrected for the difference in index of refraction of the adjoining medium.

Figures 4 and 5 show that the linear recovered and measured profiles agree within about 10 K. The second order Legendre polynomial profiles and the discrete point profiles vary more from the measured profiles than the linear recovered ones. The linear recovered profiles are expected to be the most accurate because (1) there are only two unknowns and (2) the measured profiles are nearly linear. The temperature profiles in fused silica under these conditions are essentially linear as verified analytically by Anderson *et al.* [4] and Chupp [10]. Deviations between the recovered and measured profiles are due to errors. The various sources of error are discussed in the next section.

Possible sources of error

The errors arising in the measurement of glass temperature with a Mach–Zehnder interferometer results primarily from: (1) interferometric errors due to thermal distortion and refractive effects, (2) errors in the measurement of the reference temperature and (3) errors due to the nonuniformity of temperature in the direction of the test beam. The first type of error has been accounted for in reducing the data. The reference thermocouple is attached to the bottom surface ($\xi = 1$) of the glass. This thermocouple is affected by radiation from the heater. An error analysis showed that the thermocouple junction is about 2 K higher than the surface temperature assuming perfect contact [19]. Thus, the level of the measured profile is high by 2 K.

The third type of error in the measured profile (nonuniformity of temperature in the direction of the test beam) is due to heat losses from the edges of the glass sample. The interferometric data yield an average temperature along the test beam for the glass specimen, whereas inversion determines the temperature profile near the center of the sample. Because of heat losses from the edges, it was observed that a small temperature decrease existed from the center towards the edges of the sample. Hence, the average temperature along the interferometer path is lower than at the center of the sample, and therefore the measured temperature would be lower than the recovered one. Therefore the last two types of inherent errors would cause the measured profiles to be slightly higher than the recovered profile. This could adequately explain the differences between the linear recovered and measured temperature profiles.

There are also errors in the recovered profiles. These errors are primarily of five types: (1) imprecise measure of the spectral emitted radiation, (2) computational errors due to inversion, (3) imperfect models and data for the spectral reflection and transmission characteristics of the interfaces, (4) inaccurate spectral absorption coefficient data, and (5) limited set of measured value of spectral emerging intensity. These errors could affect the temperature level of the recovered results as well as the deviation of higher order profiles.

The first type of error was minimized by carefully aligning the spectrometer to insure the maximum intensity was recorded for each test condition. Calibrating the

spectrometer with a black-body *in situ* should also minimize measurement error.

Computational errors have been extensively investigated [10]. These errors have been found to be small compared to any measurement data error.

There is some uncertainty in the reflection characteristics of interface 2. These characteristics were predicted from the Fresnel's equations of the classical electromagnetic theory using experimental index of refraction data [17]. Variation with temperature of the index of refraction for the gold and black coatings is not accurately known. The optical properties of the interfaces and hence the transmission and reflection characteristics also depend on the temperature and thus introduce small errors in the recovered profiles. In the analytical model interface 2 was assumed to be optically smooth and specularly reflecting. Examination of the coatings prior to testing showed them to be specular. However, it is uncertain whether these coatings remained specular and opaque over the range of temperature conditions during testing. Some degradation was noted at higher temperatures. The effect of error in the value of the reflectivity of interface 2 is considered in the next section. Also, the remaining types of error in the recovered profile, i.e. the effect of error in the absorption coefficient and the number of data points is presented.

Sensitivity studies

The effect of error in the various parameters was investigated by systematically perturbing the values of selected parameters and observing the effect on the recovered profiles [19]. Only results for first and second order profiles are presented.

Typical results showing the effect of the number of data points are given in Table 1. The case where $N = 10$ corresponds to that considered in Fig. 4. The data in Table 1 reveal that varying the number of data points does not greatly affect the results for $N \leqslant 10$. This is because the two unknowns are evaluated from the data being least-square fit. However, increasing N above 10 adversely affects the results. This is attributed to the fact when the number of emission data points is larger than ten, the wavelength intervals of data points are smaller than the resolution of the spectrometer (i.e. approximately 0·1 μm). Therefore, the individual points are no longer independent and errors are introduced.

Table 1. Effect of the number of emission data points on the recovered results for fused silica glass with a gold coating at the back face: $3{\cdot}66\,\mu\text{m} \leqslant \lambda \leqslant 4{\cdot}75\,\mu\text{m}$, back face temperature = 655 K

N	RMS deviation* T_{max} (%)	Average deviation* in emission data (%)
4	0·71	0·65
7	0·90	0·82
10	0·89	0·73
15	3·75	3·70

*Linear recovered profile.

The effect of varying the back surface emittance for the gold coating case is shown in Table 2. The

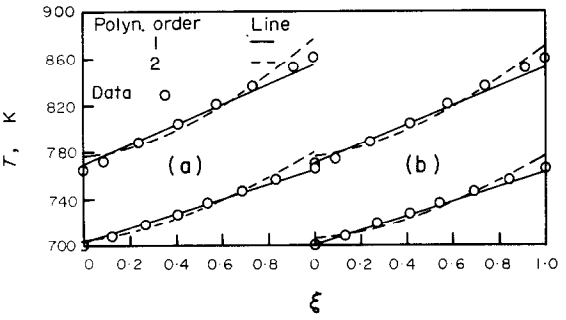

FIG. 6. Effect of back surface emittance on recovered temperature profiles using Legendre polynomial approach; Pyromark black paint at the back face, $N = 10$, $3{\cdot}66\,\mu\text{m} \leqslant \lambda \leqslant 4{\cdot}75\,\mu\text{m}$, $1{\cdot}99 \leqslant \tau_{0\lambda} \leqslant 40{\cdot}70$, (a) $\varepsilon \simeq 0{\cdot}80$ and (b) $\varepsilon \simeq 0{\cdot}88$.

Table 2. Effect of decreasing the back surface emittance on the recovered temperature profile; polynomial approach with a gold coating at the back face, $3{\cdot}66\,\mu\text{m} \leqslant \lambda \leqslant 4{\cdot}75\,\mu\text{m}$, $N = 10$ and $1{\cdot}65 \leqslant \tau_{0\lambda} \leqslant 30{\cdot}08$

	T, K				
	1st order polynomial		2nd order polynomial		
ξ	$\varepsilon_\lambda = 0{\cdot}06$	$\varepsilon_\lambda = 0{\cdot}03$	$\varepsilon_\lambda = 0{\cdot}06$	$\varepsilon_\lambda = 0{\cdot}03$	Measured
0	531·7	531·8	531·8	531·9	528·2
0·20	535·9	536·1	536·0	535·9	533·9
0·40	540·3	540·3	540·1	540·1	539·5
0·60	544·5	544·6	544·6	544·5	545·5
0·80	548·7	548·8	549·0	549·2	549·6
1·00	553·0	553·1	553·2	553·9	554·1

data in this table reveal that changing the emittance had only a small effect on the recovered temperature profiles. Decreasing the emittance slightly increased the back surface temperature and vice versa. Figure 6 shows the effect of changing the back surface emittance for the Pyromark coating case. Increasing the emittance by 10 per cent yields a slightly better agreement between the measured and recovered temperature profiles. Such an error in emittance is possible because only room temperature spectral emittance data are available for Pyromark paint [18] and the total emittance increases with temperature [20].

The influence of a uniform error in the spectral absorption coefficient data on the recovered results is shown in Fig. 7. This figure reveals that uniformly

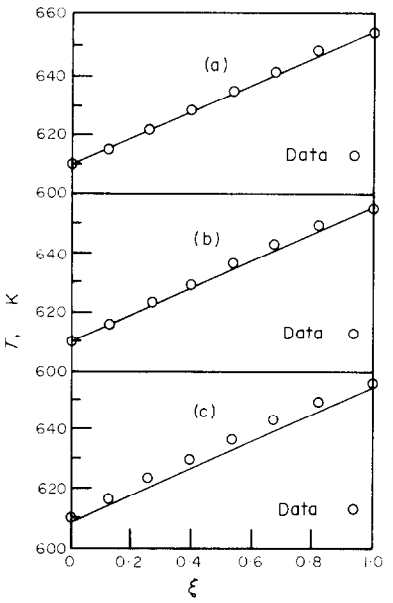

FIG. 7. Effect of spectral absorption coefficient on recovered temperature profiles using first order Legendre polynomial approximation for gold coating at the back face, $N = 10$, $\varepsilon \simeq 0{\cdot}80$, $3{\cdot}66\,\mu\text{m} \leqslant \lambda \leqslant 4{\cdot}75\,\mu\text{m}$; (a) κ_λ increased by 5 per cent ($1{\cdot}89 \leqslant \tau_{0\lambda} \leqslant 35{\cdot}09$), (b) κ_λ unchanged ($1{\cdot}80 \leqslant \tau_{0\lambda} \leqslant 33{\cdot}40$) and (c) κ_λ decreased by 5 per cent ($1{\cdot}71 \leqslant \tau_{0\lambda} \leqslant 31{\cdot}72$).

altering the absorption coefficient data by ± 5 per cent does not seriously affect the linear profile results; only the temperature level. An error in only part of the absorption coefficient data is possible. Chupp [10] has shown that correcting lower absorption coefficient values by less than 10 per cent cut the deviation of higher order profiles from the linear ones in half. This correction had only a minor effect on the linear profiles. This study then demonstrates that error in the absorption coefficient data is present but would not cause the deviations between the measured and linear recovered profiles. Accuracy of absorption coefficient data would be important for more complex temperature profiles.

Reliance on handbook data for spectral radiation properties of semitransparent materials, such as high temperature glasses, is risky when recovering more complex profiles not only because these property values are poorly known but also because small impurities (e.g. iron oxide) have very large effects on spectral absorption coefficient. For example, an error in κ_λ affects the recovered temperature near the front surface for large $\tau_{0\lambda}$, and, for smaller $\tau_{0\lambda}$, error in κ_λ affects the overall average temperature. To overcome some of these difficulties a procedure has been developed to recover the spectral absorption coefficient of the sample from the spectral emission data obtained in the experiment. In this procedure the temperature distribution is taken as known and an average (over the temperature range in the sample) spectral absorption coefficient is recovered. This information is particularly useful where data are lacking and/or large uncertainties in κ_λ exist. The details of the analysis can be found elsewhere [10].

Other investigations of the thermal remote sensing method for recovering temperature distribution in glass have been completed. The method has been used to recover nonlinear temperature profiles under dynamic conditions in a slab of clear float glass which was being cooled by convection and radiation [21]. The situation when the material is being heated by an external radiation source has also been considered and satisfactory results have been obtained [19, 21]. It is expected that the method could also be used to recover the temperature distribution in semitransparent materials when there is external radiation reflected on the top of the surface into the detector, providing the reflected radiation is accounted for in the model.

CONCLUSIONS

The results in this paper demonstrate the validity of the thermal remote sensing technique for the recovering of the temperature profile in a fused silica layer having an opaque back surface. The linear recovered profiles agree with the independently measured profiles within experimental error. Thus, the technique accurately recovers the temperature profile for the experiments performed.

Sensitivity studies show that: (1) varying the number of emission data points has only a minor effect when the number-of-unknowns-to-number-of-data-points ratio is small (providing the instrumentation spectral resolution is not exceeded), (2) error in the back surface emittance appreciably affect the recovered results for the high emittance back surface but not

for the low emittance one, and (3) error in the absorption coefficient data could explain part of the deviations of higher order profiles from the linear ones. The results showing the effect of absorption coefficient demonstrate that good property data would be needed if nonlinear temperature profiles are encountered.

The spectral thermal remote sensing method appears to have potential as a diagnostic technique for recovering temperature distribution in semitransparent condensed phases at high temperatures under both steady and dynamic conditions since it can yield detailed data (where desired) that is not possible with probes or radiation thermometry.

Acknowledgements—This research was supported, in part, by the National Science Foundation under Grant No. GK 32373X. Detroit Diesel Allison, Division of General Motors Corporation, provided support to one of the authors (R.E.C.) to continue his doctorate research in absentia. Computing facilities were made available by Purdue University Computing Center. The authors wish to thank Dr. E. E. Anderson for his advice and assistance during the initial phases of the experimental work.

REFERENCES

1. M. Nishimura, M. Hasatami and M. Sugiyama, Simultaneous heat transfer by radiation and conduction. High temperature one-dimensional heat transfer in molten glass, *Int. Chem. Engng* **8**, 739–745 (1968).
2. T. Land, Advances in glass temperature measurement, *Glass Industry* **43**, 244–247, 250–251, 282–283 (1962).
3. N. D. Eryou and L. R. Glicksman, An experimental and analytical study of radiative and conductive heat transfer in molten glass, *J. Heat Transfer* **94C**, 224–230 (1972).
4. E. E. Anderson, R. Viskanta and W. H. Stevenson, Heat transfer through semitransparent solids, *J. Heat Transfer* **95C**, 179–186 (1973).
5. J. Y. Wang, Theory and applications of inversion techniques: A review, Purdue University, School of Aeronautics, Astronautics and Engineering Sciences Report 70-6, West Lafayette, Indiana (1970).
6. R. Van Laethan, L. G. Leger, M. Boffe and E. Plumat, Temperature measurement of glass by radiation analysis, *J. Am. Ceram. Soc.* **44**, 321–332 (1961).
7. J. R. Beattie and E. Coen, Spectral emission of radiation by glass, *Br. J. Appl. Phys.* **11**, 321–332 (1961).
8. J. R. Beattie, Applying radiation pyrometry to glass manufacture, *Ceram. Age* **81**, 70–79 (1965).
9. R. E. Chupp and R. Viskanta, Thermal remote sensing of the temperature distribution in semitransparent solids: a numerical experiment, ASME Paper No. 72-HT-5 (1972).
10. R. E. Chupp, Development and experimental evaluation of a technique to determine the temperature distribution in semitransparent solids from remotely sensed spectral emission data, Ph.D. Thesis, Purdue University, West Lafayette, Indiana (1973).
11. E. M. Sparrow and R. D. Cess, *Radiation Heat Transfer*, pp. 191–265, Brooks/Cole, Belmont, Calif. (1966).
12. E. E. Anderson, Combined conduction and radiation in semitransparent solids: An experimental and analytical study, Ph.D. Thesis, Purdue University, West Lafayette, Indiana (1972).
13. W. Haufand U. Grigull, Optical methods in heat transfer, in *Advances in Heat Transfer*, edited by J. P. Hartnett and J. F. Irvine, Jr., Vol. 6, pp. 133–366. Academic Press, New York (1970).
14. J. H. Wray and J. T. Neu, Refractive index of several glasses as a function of wavelength and temperature, *J. Opt. Soc. Am.* **59**, 775–776 (1969).
15. B. Wedding, High temperature infrared transmittance of some optical materials, Research and Development Laboratories, Corning Glass Works, Corning, New York (1970).
16. O. J. Edwards, Optical transmittance of fused silica at elevated temperatures, *J. Opt. Soc. Am.* **56**, 1314–1319 (1966).
17. Landolt-Börnstein, *Eigenschaften der Materie in ihren Aggregatzustünden*, Vol. II, Teil 8, Optische Konstanten, pp. 1–12 to 1–13, Springer, Berlin (1962).
18. Y. S. Touloukian, Editor, *Thermal Radiative Properties—Coatings*, in Thermophysical Properties of Matter, Vol. 9, p. 121, MacMillan, New York (1972).
19. G. L. Groninger, Experimental verification of thermal remote sensing for measuring temperature distribution in fused silica, M.S. Thesis, Purdue University, West Lafayette, Indiana (1973).
20. J. R. Schornhorst, An analytical and experimental investigation of radiant heat exchange between simply arranged surfaces, Ph.D. Thesis, Purdue University, West Lafayette, Indiana (1967).
21. P. J. Hommert, Application of a thermal remote sensing method to measurement of temperature distribution in glass, M.S. Thesis, Purdue University, West Lafayette, Indiana (1973).

VERIFICATION EXPERIMENTALE D'UNE METHODE DE DETERMINATION A DISTANCE DE LA DISTRIBUTION DE TEMPERATURE DANS LE VERRE

Résumé—On étudie expérimentalement la détermination de la distribution de température dans le verre, à partir des données d'émission spectrale, par une méthode d'évaluation à distance. On formule un modèle analytique et on obtient la distribution de température cherchée par une procédure d'optimisation qui détermine le profil de température sous une forme polynomiale ou un ensemble de points de discrétisation. Pour évaluer la précision et la validité de la méthode, les températures calculées sont comparées à des mesures indépendantes par thermocouples de surface et par interférométrie Mach–Zender. Des résultats expérimentaux sur des éprouvettes de silice fondu (Corning Code 7940) sont obtenus avec un spectromètre Perkin–Elmer pour mesurer l'énergie spectrale transmise par l'épaisseur de verre. On considère des conditions aux limites d'opacité (émittance forte ou faible) sur la surface chauffée, et un

domaine de température allant de 500 K à 900 K. On a utilisé les données d'émission spectrale entre 3,3 et 4,8 μm pour déterminer la distribution de température. Les résultats montrent un bon accord entre les profils de température calculés et mesurés par interférométrie, la déviation maximale n'excédant jamais 2 pour cent.

EXPERIMENTELLE DURCHFÜHRUNG EINER THERMISCHEN FERNMESSMETHODE FÜR DIE ERMITTELUNG DER TEMPERATURVERTEILUNG IN GLAS

Zusammenfassung—Die thermische Fernmeßmethode für die Ermittlung der Temperaturverteilung in Glas aus spektralen Emissionsdaten wird experimentell erprobt. Ein analytisches Modell wird aufgestellt und die gesuchte Temperaturverteilung unter Verwendung eines Optimierungsschemas erhalten, welches das Temperaturprofil in Form eines Polynoms oder einer Tabelle diskreter Werte liefert.

Um die Genauigkeit und Gültigkeit der thermischen Fernmeßmethode zu beurteilen, werden die so erhaltenen Temperaturen mit unabhängigen Messungen verglichen, für welche Oberflächenthermoelemente und ein Mach-Zehnder-Interferometer verwendet werden.

Versuchsergebnisse werden für geschmolzene Silikatglasproben (Corning Code 7940) angegeben, wobei ein Perkin-Elmer-Spektrometer zur Messung der spektralen Strahlungsenergie, die von der Glasschicht abgegeben wird, Verwendung findet. An der beheizten Oberfläche des Glases wurden die Randbedingungen der Strahlungsundurchlässigkeit (bei hohen und niedrigen Emissionskoeffizienten) berücksichtigt. Der Bereich der untersuchten Temperaturen war 500 bis *ca.* 900 K. Für die Ermittlung der Temperaturverteilung in den Glasproben wurden die spektralen Emissionen im Bereich von 3,3 bis 4,8 μm herangezogen.

Die Ergebnisse zeigten eine gute Übereinstimmung zwischen den so ermittelten und den interferometrisch gemessenen Temperaturprofilen, wobei die maximale Abweichung niemals über *ca.* 2% lag.

ЭКСПЕРИМЕНТАЛЬНАЯ ПРОВЕРКА ТЕПЛОВОГО ДИСТАНЦИОННОГО ЧУВСТВИТЕЛЬНОГО МЕТОДА ВОССОЗДАНИЯ РАСПРЕДЕЛЕНИЯ ТЕМПЕРАТУРЫ В СТЕКЛЕ

Аннотация — В работе экспериментально исследуется тепловой дистанционный чувствительный метод распределения температуры в стекле по данным спектрального излучения. Сформулирована аналитическая модель и получено искомое распределение температуры с помощью схемы оптимизации, которая определяет температурный профиль в виде полинома или совокупности дискретных точек. Для оценки точности и справедливости дистанционного метода воссоздаваемые температуры сравниваются с результатами независимых измерений, проводимых при помощи поверхностных термопар и интерферометра Маха-Цендера. Приводятся результаты экспериментов для образцов из кварцевого стекла (Corning Code 7940) по измерению спектральной энергии излучения образцов, полученные с помощью спектрометра Перкина-Эльмера. Рассматривались непрозрачные (с высокой и низкой лучеиспускательной способностью) граничные условия на нагретой поверхности стекла. Изучались температуры в диапазоне от 500 К до 900 К. Для воссоздания распределения температуры в стеклянных образцах использовались данные спектрального излучения в диапазоне 3,3–4,8 *μm*. Результаты эксперимента показали, что воссоздаваемые и полученные с помощью интерферометра температурные профили хорошо согласуются с максимальным отклонением около двух процентов.